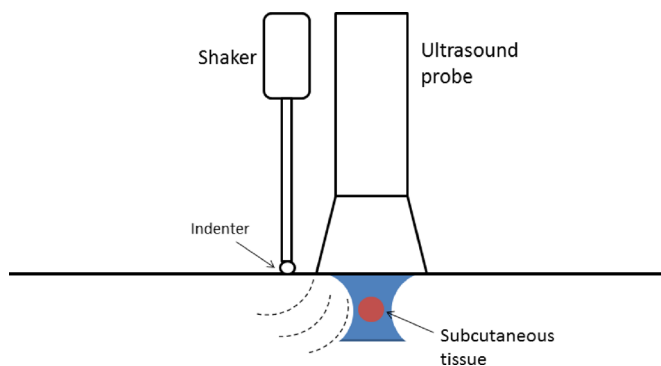


## A Clinical Pilot Study

Pedro Ciudad, MD, PhD,<sup>e</sup> Antonio J. Forte, MD, PhD, MS,<sup>b,f</sup>  
Xiaoming Zhang, PhD,<sup>c</sup> and Oscar J. Manrique, MD, FACS<sup>a,b</sup>

Copyright © 2020 Wolters Kluwer Health, Inc. All rights reserved.



**FIGURE 1.** Schematic of the generation and detection of the shear wave using UVE. A shaker is acting on the tissue surface. An ultrasound probe monitors the wave in the tissue. [full color online](#)

assess skin, subcutaneous connective tissue, and muscle. There is a need for quantitative measurement to effectively evaluate disease development and monitor treatments. We hypothesize that the degree of stiffening subcutaneous tissue due to secondary lymphedema in the extremity could be noninvasively assessed in terms of relative difference in shear wave speed between affected and control limbs. This clinical pilot study was aimed at detecting differences between lymphedematous and nonlymphedematous extremities using UVE and potentially translating an UVE into clinical use for quantitative assessment of patients with secondary lymphedema of the extremity.

## MATERIALS AND METHODS

### Study Population

This clinical pilot study was approved by the Mayo Clinic Institutional Review Board (study ID: 18-009694). Each patient completed a written, informed consent form and the rights of each subject were protected. We performed a pilot study recruiting adult patients with clinical and lymphoscintigraphic diagnosis of lymphedema between March and April 2019. Patients with history of surgical treatment for lymphedema were excluded. Diagnosis of lymphedema was based on

clinical history, physical examination and lymphoscintigraphic imaging showing either interruption of lymphatic flow, dermal backflow, delayed flow, or delayed visualization or nonvisualization of lymph nodes or lymphatic system.<sup>12</sup> Other causes of extremity edema, such as congestive heart failure or chronic venous insufficiency, were ruled out with the use of other diagnostic tools, such as conventional Doppler ultrasound, if clinical suspicion was high. We used 3 anatomic landmarks for measurement: 10 cm above ankle/wrist, and 10 cm above and below knee/elbow. Participants were tested in a supine position with their extremities placed horizontally on a pillow in a relaxed state.

### Study Protocol: UVE

The indenter of the handheld shaker was placed on the tissue. A 0.1 s harmonic vibration was generated by the indenter of the handheld shaker (Model FG-142; Labworks, Costa Mesa, CA) on the tissue.<sup>13,14</sup> The vibration was generated at 3 frequencies: 100, 150, and 200 Hz.<sup>15</sup> Tissue motion was in response to the external vibration excitation induced by the handheld vibrator.<sup>16,17</sup> A Verasonics ultrasound system (Verasonics Vantage; Verasonics, Kirkland, WA) with an L11-5v ultrasound probe with a central frequency of 6.4 MHz was positioned about 5 mm away from the indenter and used for detecting shear wave motion of the tissue (Fig. 1).<sup>18</sup> Images of the tissue were acquired by compounding 11 successive angles at a pulse repetition frequency of 2 kHz.<sup>19,20</sup> Three measurements were performed at each location and at each frequency. Both normal and affected extremities were measured. Typical testing lasted about 10 minutes.

### Image Analysis

Particle velocity in the axial direction (V) caused by wave propagation was used for wave speed estimation. V was calculated from in-phase/quadrature (IQ) data of consecutive frames using a 1-dimensional autocorrelation method.<sup>21,22</sup> Sound speed (c) was assumed to be 1540 m/s. Pulse repetition frequency was 2000 pulses per second. Central frequency (f) was 6.4 MHz. Three pixels in the axial direction and 2 sampling points in the slow time direction were used for averaging. A  $3 \times 3$  pixel spatial median-filter was then used on each frame of the wave motion image to remove noise spike points. Shear wave speed measurement is performed by cross-correlating 2 particle velocities from 2 imaging pixels.<sup>22,23</sup>

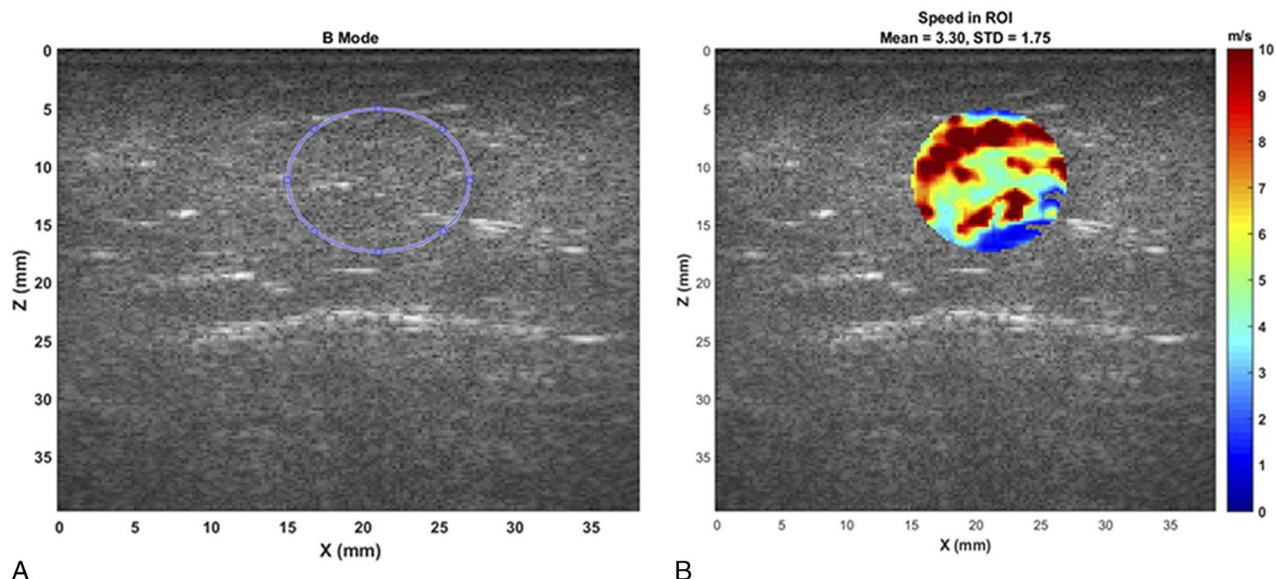


**FIGURE 2.** (A,) Representative ROI in subcutaneous tissues and (B) corresponding measured shear wave speed. [full color online](#)

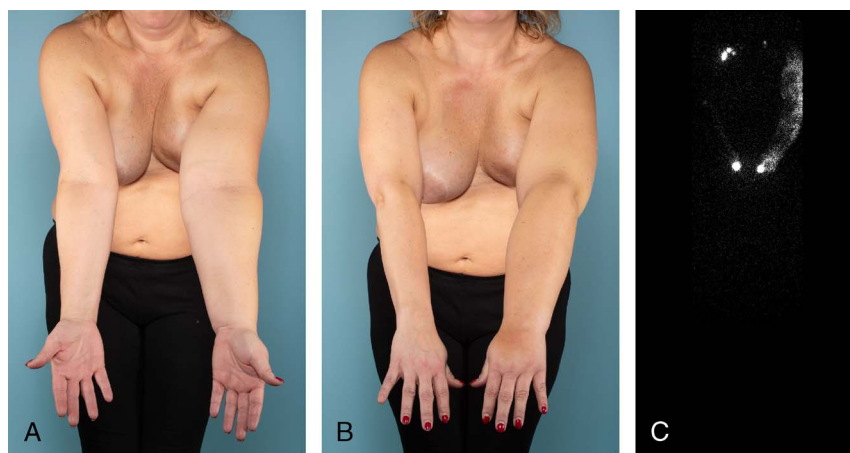


**FIGURE 3.** Images (A) and (B) show a 49-year-old female patient with a BMI of 31.2 kg/m<sup>2</sup> that started developing swelling and aching pain of her left upper extremity for almost 2 years. The symptoms started after undergoing left breast conserving surgery with lumpectomy, radiation therapy and axillary lymph node dissection. A lymphoscintigraphic imaging 3 hours after radiotracer injection evidencing delayed lymphatic drainage and dermal backflow in her left upper extremity is shown in the image (C). [full color online](#)

To increase the robustness of the 2D shear wave speed calculation while preserving the spatial resolution of the shear wave speed map, a 2D processing window technique was used.<sup>24,25</sup> In the 2D window processing technique, all pixels within the 2D window are used to estimate shear wave speeds along the axial and lateral directions. A sliding patch that is smaller than the window size was used to calculate normalized cross-correlations between each pair of shear wave signals at spatial locations that are  $p$  pixels apart. A window size of 12 and patch size of 9 were used throughout this study.

Via iterating the calculations through all imaging pixels, a 2D shear wave speed map can be obtained. A region of interest (ROI) was selected to measure wave speeds of subcutaneous tissues in one piece and the corresponding wave speed of the ROI was calculated (Fig. 2). Wave speed of the ROI is a combination of both the axial and lateral speed. Therefore, it is an absolute wave speed at each pixel.

### Statistical Analysis

A 2-tailed Wilcoxon rank-sum test ( $P < 0.05$ ) was conducted to compare sample medians between control and lymphedema sites.

### RESULTS

Eleven patients with secondary lymphedema (6 with upper limb and 5 with lower-limb lymphedema) from the Mayo Clinic Division of Plastic and Reconstructive Surgery were enrolled. All were female. We excluded patients who had surgery for the treatment of lymphedema. Based on the International Society of Lymphology staging system, 3 were stage I, whereas 8 were stage II-III. The median age of the patients was 57 years (48–74 years), and the median body mass index was 28.9 kg/m<sup>2</sup> (19.3–42 kg/m<sup>2</sup>). Five patients developed lower-extremity lymphedema after endometrial cancer treatment and one after cervical cancer treatment; six patients developed upper extremity breast cancer-related lymphedema. Median time of lymphedema-associated symptoms was 2 years (1–20 years). Figure 3 depicts one clinical case included in this study. Clinical and lymphoscintigraphic images are shown.

When analyzing the subcutaneous tissue as a whole, the magnitudes of the shear wave speeds of subcutaneous tissues at 100, 150 and 200 Hz at lymphedema sites ( $4.14 \pm 0.16$  m/s,  $4.98 \pm 0.75$  m/s, and  $5.85 \pm 0.62$  m/s) were statistically higher than those of the control sites ( $2.31 \pm 0.13$  m/s,  $2.84 \pm 0.32$  m/s, and  $3.29 \pm 0.44$  m/s) ( $P < 0.05$ ) (Fig. 4). Figure 5 shows the shear wave speeds of the ROI in the subcutaneous tissue of control and lymphedema sites of patients with

lymphedema in the upper extremity or lower extremity at 100, 150, and 200 Hz. The magnitudes of the wave speeds of the ROI in the subcutaneous tissue at lymphedema sites in the upper extremity ( $3.9 \pm 0.17$  m/s,  $5.96 \pm 0.67$  m/s, and  $7.41 \pm 1.09$  m/s) were statistically higher than those of the control sites ( $2.1 \pm 0.27$  m/s,  $2.93 \pm 0.57$  m/s, and  $3.56 \pm 0.76$  m/s) at 100, 150, and 200 Hz ( $P < 0.05$ ). There was a statistically significant difference in the shear wave speed of the ROI in the subcutaneous tissue at 100 and 200 Hz ( $P < 0.05$ ) between lymphedema ( $4.33 \pm 0.35$  m/s,  $4.17 \pm 1.00$  m/s, and  $4.56 \pm 0.37$  m/s) and controls sites ( $2.48 \pm 0.43$  m/s,  $2.77 \pm 0.55$  m/s, and  $3.06 \pm 0.29$  m/s) in the lower extremity.

### DISCUSSION

The aim of this study was to translate an UVE technique into clinical use for quantitative assessment of patients with secondary lymphedema of extremity. Shear wave speeds of both the control and lymphedema sites were measured. The shear wave speed of the subcutaneous tissue was measured by analyzing ultrasound data directly from the tissue. Hence, the measurement of shear wave speed was local and independent of the location and amplitude of excitation. The relative difference in terms of shear wave speed between the affected

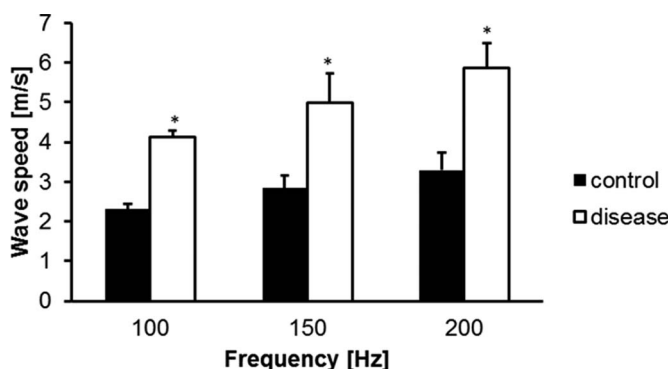


**FIGURE 4.** Comparison of shear wave speed of the ROI in subcutaneous tissue at 3 frequencies between control and lymphedema sites of the patients at upper extremity or lower extremity.



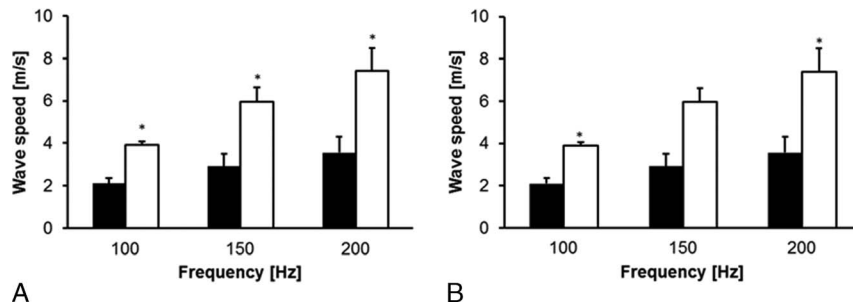


**FIGURE 5.** Comparison of shear wave speeds of the region of interest (ROI) in subcutaneous tissues at 3 frequencies between control and lymphedema sites for patients at upper extremity (A) or lower extremity (B).

and controlled extremity could be used for evaluating the severity of secondary lymphedema.

The obtained results in this study were in agreement with reported results in literature. We found that the wave speed of subcutaneous tissue at the lymphedema sites was statistically higher than that of control sites. It has been shown that there is a statistically significant difference in the elastography measurements between normal forearm and forearm with lymphedema.<sup>25</sup> Skin and subcutaneous tissue strains were lower in legs with symptomatic lymphedema at an advanced stage.<sup>26,27</sup> Chan, et al used acoustic radiation force impulse elastography to assess the limb lymphedema and reported that shear wave velocity was significantly higher in limbs with lymphatic obstruction than in unaffected limbs.<sup>28</sup> The secondary lymphedema could affect not only subcutaneous tissue but also subfascial tissue. To generate sufficient motion in the subfascial tissue using radiation force, a relatively high-intensity ultrasound field is needed. This may raise safety issue and cause tissue damage. One advantage of UVE is that the shear wave is locally generated by a mechanical shaker and diagnostic ultrasound is only used for detecting shear wave propagation in the tissue. Hence, UVE is a safe technique for subfascial tissue testing and assessing patients.

Optical coherence tomography (OCT) and OCT-based elastography techniques provide high-spatial resolution of skin tissue, yet are unable to measure deep subcutaneous tissue.<sup>29–31</sup> The imaging penetration of OCT in skin can be up to 1.5 mm.<sup>32</sup> Lymphedema affects not only skin, but also subcutaneous tissue. One advantage of UVE is its ability to evaluate wave speed of the subcutaneous tissue. In the current experimental setup, subcutaneous tissue can be measured up to 45 mm (Fig. 2). The repeatability and reproducibility of the UVE measurements on the upper extremity were evaluated in our previous study.<sup>11</sup> Interclass correlation coefficients of interrater reliability were 0.94, 0.96, and 0.98 for wave speeds at 100, 150, and 200 Hz, respectively as well as the interclass correlation coefficients of intrarater reliability were 0.95, 0.91, and 0.95. This shows that the UVE is reliable for evaluating the shear wave speed of subcutaneous tissue.

The reason to generate vibration at three different frequencies is that the shear elasticity and viscosity of subcutaneous tissue can be calculated using Voigt's model based on measurements of shear wave speeds at three frequencies and tissue density. However, the density of subcutaneous tissue of affected and control extremities was not evaluated in this study. In the future, we will develop a technique to noninvasively measure the subcutaneous tissue density and use Voigt's model to grade the severity of secondary lymphedema based on its viscoelasticity of subcutaneous tissue.

There are several limitations in this pilot study that should be considered in the interpretation of the obtained results. This is a pilot study, which is understood as a small study done to assist the preparation of a larger, more comprehensive study.<sup>33</sup> It was designed to provide preliminary evidence on the feasibility of UVE for detecting a difference in extremities with lymphedema compared with extremities with

normal lymphatic flow and drainage. With the data of this pilot study, we have now started a larger, full-scale study to further validate these results before acceptance and routine implementation of this technology as an additional diagnostic tool for lymphedema. We neglected the effect of the initial pressure to the skin, which might affect the results among different patients. The ultrasound transducer was placed onto the skin and ultrasound transmission gel was applied between the skin and ultrasound transducer for better transmission quality. The ultrasound transducer was in touch with the ultrasound gel to acquire the ultrasound image, and we tried our best to make sure the pressure applied to the skin was negligible so as not to affect our measurement of wave speed. However, we may study it by carefully adjusting the generated pressure on the skin and measuring the associated wave speed changes. This can be used for assessing nonlinearity or hyper-elasticity of skin tissue. We acknowledge the importance of the assessment of lymph flow evaluation (lymphoscintigraphy or other lymphographic studies) for the diagnosis and evaluation of lymphedema. However, the pathophysiologic effect of lymphedema in the subcutaneous tissue may be used by UVE as an indirect measurement of lymphedema, and it may become another available tool in the diagnostic armamentarium of lymphedema.

## CONCLUSION

Ultrasound vibroelastography provides a noninvasive and non-ionizing technique to assess the shear wave speed of subcutaneous tissue for patients with secondary lymphedema of extremity. These preliminary data suggest that the magnitudes of wave speed of lymphedema sites were significantly higher than those of the control sites making this tool useful in the evaluation of patients with secondary lymphedema. Based on these data, a study with a larger cohort of patients is currently in process to validate these results.

## ACKNOWLEDGMENTS

The authors thank Ms. Jennifer Poston for editing this manuscript.

## REFERENCES

1. Meneses KD, McNeas MP. Upper extremity lymphedema after treatment for breast cancer: a review of the literature. *Ostomy Wound Manage.* 2007;53:16–29.
2. Podratz KC, Symmonds RE, Taylor WF, et al. Carcinoma of the vulva: analysis of treatment and survival. *Obstet Gynecol.* 1983;61:63–74.
3. Gould N, Kamelle S, Tillmanns T, et al. Predictors of complications after inguinal lymphadenectomy. *Gynecol Oncol.* 2001;82:329–332.
4. Beesley V, Janda M, Eakin E, et al. Lymphedema after gynecological cancer treatment: prevalence, correlates, and supportive care needs. *Cancer.* 2007; 109:2607–2614.
5. Abu-Rustum NR, Alektiar K, Iasonos A, et al. The incidence of symptomatic lower-extremity lymphedema following treatment of uterine corpus malignancies: a 12-year experience at Memorial Sloan-Kettering Cancer Center. *Gynecol Oncol.* 2006;103:714–718.
6. Mortimer PS. The pathophysiology of lymphedema. *Cancer.* 1998;83(12 Suppl American):2798–2802.

7. Cormier JN, Askew RL, Mungovan KS, et al. Lymphedema beyond breast cancer: a systematic review and meta-analysis of cancer-related secondary lymphedema. *Cancer*. 2010;116:5138–5149.
8. Sander AP, Hajer NM, Hemenway K, et al. Upper-extremity volume measurements in women with lymphedema: a comparison of measurements obtained via water displacement with geometrically determined volume. *Phys Ther*. 2002;82:1201–1212.
9. Armer JM. The problem of post-breast cancer lymphedema: impact and measurement issues. *Cancer Invest*. 2005;23:76–83.
10. Zhang X, Zhou B, Kalra S, et al. An ultrasound surface wave technique for assessing skin and lung diseases. *Ultrasound Med Biol*. 2018;44:321–331.
11. Zhang X, Zhou B, Kalra S, et al. *Quantitative assessment of scleroderma using ultrasound surface wave elastography*. Ultrasonics Symposium (IUS), 2017 I.E. International; 2017:1–3.
12. Zhang X, Osborn T, Zhou B, et al. Lung ultrasound surface wave elastography: a pilot clinical study. *IEEE Trans Ultrason Ferroelectr Freq Control*. 2017;64:1298–1304.
13. Kubo K, Zhou B, Cheng YS, et al. Ultrasound elastography for carpal tunnel pressure measurement: a cadaveric validation study. *J Orthop Res*. 2018;36:477–483.
14. Sit AJ, Kazemi A, Zhou B, et al. Comparison of ocular biomechanical properties in normal and glaucomatous eyes using ultrasound surface wave elastography. *Invest Ophthalmol Vis Sci*. 2018;59:1218.
15. Zhou B, Zhang X. Comparison of five viscoelastic models for estimating viscoelastic parameters using ultrasound shear wave elastography. *J Mech Behav Biomed Mater*. 2018;85:109–116.
16. Cheng Y-S, Zhou B, Kubo K, et al. Comparison of two ways of altering carpal tunnel pressure with ultrasound surface wave elastography. *J Biomech*. 2018;74:197–201.
17. Clay R, Bartholmai BJ, Zhou B, et al. Assessment of interstitial lung disease using lung ultrasound surface wave elastography: a novel technique with clinicoradiologic correlates. *J Thorac Imaging*. 2018.
18. Zhou B, Zhang X. The effect of pleural fluid layers on lung surface wave speed measurement: experimental and numerical studies on a sponge lung phantom. *J Mech Behav Biomed Mater*. 2019;89:13–18.
19. Zhang X, Zhou B, Osborn T, et al. Lung ultrasound surface wave elastography for assessing interstitial lung disease. *IEEE Transact Biomed Eng*. 2018;1.
20. Kasai C, Namekawa K, Koyano A, et al. Real-time two-dimensional blood flow imaging using an autocorrelation technique. *IEEE Transac Sonics Ultrasonics*. 1985;32:458–464.
21. Zhang X, Zhou B, Miranda AF, et al. A novel noninvasive ultrasound vibro-elastography technique for assessing patients with erectile dysfunction and Peyronie disease. *Urology*. 2018;116:99–105.
22. Tanter M, Bercoff J, Athanasiou A, et al. Quantitative assessment of breast lesion viscoelasticity: initial clinical results using supersonic shear imaging. *Ultrasound Med Biol*. 2008;34:1373–1386.
23. Zhou B, Chen JJ, Kazemi A, et al. An ultrasound vibro-elastography technique for assessing papilledema. *Ultrasound Med Biol*. 2019;45:2034–2039.
24. Anderssen R, Hegland M. For numerical differentiation, dimensionality can be a blessing! *Math Comput Am Math Soc*. 1999;68:1121–1141.
25. Song P, Manduca A, Zhao H, et al. Fast shear compounding using robust 2-D shear wave speed calculation and multi-directional filtering. *Ultrasound Med Biol*. 2014;40:1343–1355.
26. Erdogan Iyigun Z, Agacayak F, Ilgun AS, et al. The role of elastography in diagnosis and staging of breast cancer-related lymphedema. *Lymphat Res Biol*. 2019;17:334–339.
27. Suehiro K, Morikage N, Murakami M, et al. Skin and subcutaneous tissue strain in legs with lymphedema and lipodermatosclerosis. *Ultrasound Med Biol*. 2015;41:1577–1583.
28. Suehiro K, Nakamura K, Morikage N, et al. Real-time tissue elastography assessment of skin and subcutaneous tissue strains in legs with lymphedema. *J Med Ultrason*. 2014;41:359–364.
29. Chan W-H, Huang Y-L, Lin C, et al. Acoustic radiation force impulse elastography: tissue stiffness measurement in limb lymphedema. *Radiology*. 2018;289:759–765.
30. Abignano G, Buch M, Emery P, et al. Biomarkers in the management of scleroderma: an update. *Curr Rheumatol Rep*. 2011;13:4–12.
31. Li C, Guan G, Zhang F, et al. Laser induced surface acoustic wave combined with phase sensitive optical coherence tomography for superficial tissue characterization: a solution for practical application. *Biomed Opt Express*. 2014;5:1403–1419.
32. Nguyen TM, Song S, Arnal B, et al. Shear wave pulse compression for dynamic elastography using phase-sensitive optical coherence tomography. *J Biomed Opt*. 2014;19:16013.
33. Liang X, Boppart SA. Biomechanical properties of in vivo human skin from dynamic optical coherence elastography. *IEEE Trans Biomed Eng*. 2010;57:953–959.